

VIRTUAL FLIGHT TESTING WITH VIRTAC-CASTOR: NEW CAPABILITIES AND FLIGHT ENVELOPE DEFINITION

C. Deiler, N. Fezans

DLR (German Aerospace Center), Institute of Flight Systems

Lilienthalplatz 7, 38108 Braunschweig, Germany

Abstract

This paper presents the newest release (v0.52-beta) of the VIRTAC-Castor flight dynamical simulation model. VIRTAC-Castor is the first model of a larger family, VIRTAC (Virtual Test Aircraft), developed at the DLR Institute of Flight Systems and freely available on GitHub. These models are black boxes in order to put the users in the situation of a flight test engineer who does not have access to the model equations or parameters but can only test the complete aircraft system as a whole. The VIRTAC-Castor configuration is a 100-passenger twin-engine high-wing T-tail transport aircraft. The novelties introduced with this new version include the first versions of two fault/abnormal scenarios: a wing icing case and actuator jamming for one or more primary control surfaces (elevators, ailerons, or rudder). In addition to introducing these new features, the paper also provides new information regarding the operational flight envelope (e.g. service ceiling, VMO, MMO, VFE for each configuration).

1 VIRTAC: VIRTUAL TEST AIRCRAFT – MOTIVATION AND OBJECTIVES

The authors recently started developing and sharing on GitHub a family of aircraft models called VIRTAC¹ (Virtual Test Aircraft). The whole idea of creating VIRTAC comes from the observation of the authors that in the area of flight dynamics and flight control there is a lack of commonly available, good and realistic benchmark models close to real aircraft behavior and characteristics. Most engineers and researchers are developing and/or using proprietary models for their work, but they often cannot share these models. Very often these restrictions result from the vehicles themselves and the fact that manufacturers tend to consider that these models might reveal some trade secrets or that they might lose some control over the investigations made based on the models of their vehicles. Engineering-related disciplines differ from more fundamental science in the sense that their actual goal is less to produce new knowledge than to create something of economical or strategic value from the current body of knowledge. Whilst new knowledge might be produced along the way, the context strongly drives engineering work towards a future return on investment. In this context, openness is mainly seen as a potential future loss of revenue and as potentially endangering the currently foreseeable revenues (e.g. through additional risks to current programs). In order to support research and science in their domains,

the authors decided to build and provide VIRTAC to the entire community.

Valuable research can be done using proprietary models and published, but the comparison of the results obtained is very difficult since each scientist not only might have tuned their method/system slightly differently but also have very different applications/models to start with. For example, in 17 fairly recent publications related to aircraft flight envelope protections [1–17] no less than 12 different aircraft types or models were used. Similarly, publications on system identification of flight systems also have been explained and demonstrated using numerous aircraft, e.g. no less than 20 different aircraft types are considered in the references [18–36].

Apart from slowing down research and innovation, this situation is also problematic in the sense that good science thrives through comparing hypotheses with observations and through independent validation of the results by different teams. Reproducibility of the results and cross-checking have been corner stones in science and will remain so. Note that it is a fundamental problem across all scientific areas. In order to foster research in mathematical optimization, many test functions have been developed and commonly used to illustrate the properties of optimization methods (see for instance [37] and references therein). In aeronautics, various examples of commonly shared benchmark problems can be found as well. For instance, NASA have developed and shared the "Common Research Model" (CRM) and the "Transport Class Model" (TCM). CRM is an aircraft configuration for which data has been produced and shared.

¹<https://github.com/VIRTAC/VIRTAC>
Contact: VIRTAC@dlr.de

In particular application to high speed, natural laminar flow, and icing can be found in the literature. TCM is derived from a sub-scale “Generic Transport Model” (GTM) simulation [38] and is a fully functioning aircraft flight dynamics simulation including realistic engine and actuator behavior, sensor models and a flight control system. Although a significant number of failure scenarios were considered, computed and tested in CFD and wind tunnels [39], only a few of them were implemented in the distributed Simulink simulation model.

VIRTTAC is developed to address this problem with two main objectives in mind:

1. provide high-quality representative models to engineers and researchers who need some but do not have access to the kind of research infrastructure that the authors have access to.
2. provide a wide range of benchmarks to the community with various complexity levels, including some which comprise as many real-world effects as possible. The objective for the most complex benchmarks is that it should never be possible to pass them successfully but fail in the real-world due to effects that could not be tested with VIRTTAC. Whilst the objective is to build complete benchmarks, the current work mainly focuses on the development of the dynamic aircraft model at the heart of these benchmarks. A first benchmark example for aircraft system identification is presently being developed [40].

This last element “never pass the most complex benchmark if it fails in practice” directly leads to the need for representative system architectures and for modeling of all kinds of real-world effects. Information that would not be available in practice should also be hidden from the users of VIRTTAC in order to ensure that it cannot be exploited. This includes information on the internal working of the models, their exact structure, parameter values, etc. Similarly, all values that are required for performing the simulations but which would not be available in practice (e.g. information for which no sensor exists or is installed/available in a real aircraft) are not accessible to the users. To some extent, VIRTTAC might be compared to TCM as they both provide flight dynamics simulation models, but there are two major differences: First, as it will become clearer in the following, VIRTTAC will progressively include more than just the simulation model. Second, as just explained, the internal working of the VIRTTAC model also needs to be hidden from the users.

Most users have prior knowledge about flight mechanics/dynamics and control and they should use it. The behavior of VIRTTAC will be very familiar to flight dynamics specialists, since the vehicle behaves like an aircraft. However, no equations and no aerodynamic coefficient derivatives will be made available. Precise knowledge of the aircraft can be gained by “virtually flight-testing”

it (i.e. performing simulations with the same constraints as in flight test). Knowledge gained on the VIRTTAC models can be exchanged with the rest of the community (e.g. through exchange of models obtained through system identification) and is encouraged. The authors intend, aside from the website where VIRTTAC and its updates can be downloaded, to organize with the interested parties an exchange platform for the community and gather information regarding all investigations that were performed using VIRTTAC. If users want to share such models or data related to one of the VIRTTAC models, they can either make a “pull request” within the GitHub platform or contact the VIRTTAC team under the e-mail address: VIRTTAC@dlr.de.

In the long term, the authors plan to build several models with slightly different characteristics and behaviors. For each of these models a rough description of the model will be provided. This description will include some basic description of the shape of the aircraft and its geometry and can be imagined as what a specialist would notice by looking at the aircraft. A few key technical specifications will be provided as well. It is not intended to enable users to generate alternative data sets on the aircraft from other sources than the provided simulation model, therefore no detailed design data of any kind will be provided (no CAD geometry, structure design, etc.). The simulation is based on a nonlinear rigid-body model, which is meant to be valid for a predefined flight envelope and will include several high-lift configurations and additional effects like stall or ground effect in its final version.

The only aircraft considered hereafter is named VIRTTAC-Castor, the first of the VIRTTAC family [41].

2 OVERVIEW OF VIRTTAC-CASTOR

VIRTTAC-Castor represents a generic short- to medium-haul transport aircraft for around 100 passengers with a high wing (small anhedral) and a T-tail configuration. This configuration has been completely created from scratch for VIRTTAC [41]. An artistic illustration of the VIRTTAC-Castor is given in Fig. 1 and as well in Fig. 2 as three-side view. This illustration is provided for a common understanding of the modeled aircraft but no CAD model and precise geometry is given/distributed (at least for now). This aircraft was not produced through a complete pre-design process but its dimensions and characteristics correspond to a short-to-medium range commercial air transportation role with a capacity of around 100 passengers. Table 1 provides an overview on its current dimensions and characteristics, which is not complete but gives the user the necessary information for subsequent model use.

Aerodynamics:

The aircraft model's aerodynamics contain formulations of nonlinear and unsteady effects of wing and empen-



Figure 1: Artistic illustration of the VIRTAC-Castor configuration

Geometry

aircraft length	30.0 m
wing span	28.0 m
horizontal tail span	10.4 m
wing area	75.0 m ²
horizontal tail area	20.0 m ²
wing aspect ratio	10.4
mean aerodynamic chord	2.17 m

Main characteristics

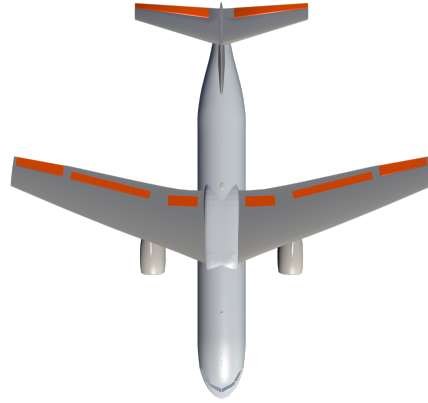
MTOW / max. take-off weight	56 000 kg
empty weight	33 000 kg
max. fuel weight	16 000 kg
max. payload / PAX weight	12 000 kg
max. range	5 500 km
service ceiling	35 000 ft
MMO / max. operating Mach number	0.76
VMO / max. operating speed	300 kt CAS
cruise Mach number	0.725

Table 1: Key parameters of VIRTAC-Castor

nage. The model benefits from DLR's large experience in modeling and identifying complex aerodynamic models for different airplanes across their full flight envelope [24, 42, 43]. The aerodynamic model formulation allows easy implementation of failure cases of an aerodynamic degradation of various sources as defined in section 5.

Propulsion:

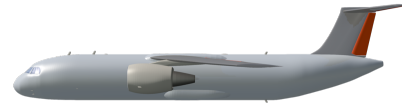
The VIRTAC-Castor model further includes two turbofan engine models which can be controlled separately. The engine command inputs correspond to a engine fan shaft rotation speed N_1 expressed in % of the nominal maximum speed. The dynamic model will therefore correspond to the behavior of the engine plus the corresponding FADEC. The long term development of VIRTAC-Castor will include the implementation of complex dynamic models of the engines, but for the first version of VIRTAC-Castor only much simpler preliminary



(a) top view



(b) front view



(c) side view

Figure 2: Artistic illustration of the VIRTAC-Castor configuration, multiview projection

models will be used to describe the engine characteristics.

Flight Controls:

The simulation model of VIRTAC-Castor contains several control surfaces including various spoilers on the wing. In detail, the model provides:

- trimable horizontal stabilizer
- left and right elevators
- left and right ailerons
- rudder
- five spoilers on each side (four roll spoilers/airbrakes and one ground spoiler)

Actuator models are implemented for all control surfaces including limits for deflections, deflection rates, and accelerations. The actual control surface deflection is measured internally by the actuator and provided as output of the VIRTAC-Castor model. The commanded signal and the measured deflection can therefore be compared, enabling the users to compare them within a flight control system fault detection logic. Different actuator faults will be integrated in the model over time (see section 5).

Sensor Models:

Sensor models are a crucial element for VIRTAC: they are the only way to know what is happening to the aircraft during the simulation. The physical quantities measured, the sensor characteristics (e.g. calibration, noise, dynamic behavior, quantization errors) as well as all the real-world issues related to where and how they are installed on the airframe are defined as closely as possible to the state-of-the-art regular aircraft instrumentation. The usual list of measurements provided by air data and inertial reference systems on Part/CS-25 airplanes is available for VIRTAC(-Castor). When it is common practice to have redundancies in the regular aircraft instrumentation, several sensors are also modeled. For now, VIRTAC-Castor² contains three inertial reference units and four independent air data systems.

3 UPDATED VERSION VIRTAC-CASTOR, VERSION 0.52-BETA

The first version of VIRTAC-Castor, version 0.5-alpha, was announced and briefly described in [41, 44] and put on GitHub in May 2019, and since then a few bug fixes have been integrated to this version. It is available for Windows, Mac OS, and Linux and successfully tested with a wide range of MATLAB/Simulink versions. The new features described in the following of the present paper constitute the modifications between the versions 0.5-alpha and 0.52-beta of VIRTAC-Castor. The descriptions given hereafter are restricted to the changes that can be observed by the users: the purely internal modifications to the source code of the model and of the simulation framework are not described hereafter.

The aircraft trim algorithm never perfectly trims the aircraft. This is intended because in practice test pilots try to establish the set of flight conditions defined for the test point and described on the corresponding test card, but these conditions are never perfectly established. Regardless of the motivations for performing this test point and the actions that are then undertaken (e.g. exciting the aircraft for system identification or activating a new flight controller), the final result should be robust against the imperfect initial conditions. The deviations from the desired flight conditions are taken randomly within reasonable bounds. The exact same simulation cannot be performed twice (the seed of the random generator is initialized differently to prevent this), just as a given test point cannot be reproduced under exactly the same conditions (same mistrim and atmospheric turbulence). In order to ease debugging tasks, the development of a special mode avoiding this limitation is considered by the authors, but to which extent this functionality will be provided for end users of VIRTAC remains unclear for now. Furthermore, from this new version on (0.52-beta), VIRTAC-Castor will always fly within a at least very

lightly turbulent atmosphere. The authors have a quite extensive list of ideas to make a more realistic modeling of the atmosphere and to include it in future versions of VIRTAC-Castor. However, many improvements regarding the VIRTAC-Castor model itself (flight dynamics, aerodynamics, systems, etc.) are of higher priority for now and therefore little to no improvement related to the model of the atmosphere used shall be expected in the near future.

Moreover, with VIRTAC-Castor 0.52-beta a few new, yet still incomplete, features regarding aircraft loading and the fuel management are added. VIRTAC-Castor now includes three separate fuel tanks (one in the left wing, one in the right wing and one center tank) with the respective capacities given in Table 2. The external user-defined set of fuel quantity resp. fuel mass is replaced by the definition of a fuel configuration, which further defines the fuel quantity in each tank (even distribution) and the corresponding change of the center of gravity (CG). During the flight, fuel is consumed from the tanks and the weight and balance of the aircraft changes accordingly with the simulation time. With the implementation of this new weight and balance configuration, new sensors for fuel flow and fuel quantities in each tank have been implemented and their outputs are now part of the vector of measurements provided in the outputs of the model. These changes in the weight and balance implementation brings VIRTAC-Castor one step closer to its foreseen realism, but a complete simulation of a real fuel system architecture is not included yet.

Users can now provide their own payload and payload mass distribution. Presently, a payload mass as well as a payload center of gravity (CG) position³ can be selected. In order to prevent mistakes, basic checks are implemented. For instance, the sum of the masses of the empty aircraft, the fuel, and the payload are not allowed to exceed the maximum take-off weight (MTOW). The payload cannot have negative mass either. Presently the payload CG cannot lie outside the fuselage or even unrealistically close to the fuselage limits. Adding masses outside the fuselage might be considered later on, e.g. for wing pods, but this kind of features is likely to remain of low priority.

A complete loading (weight & balance) envelope still needs to be defined for VIRTAC-Castor. It would include the typical limits on the longitudinal and lateral CG position which results from stability and controllability requirements. Eventually, limits related to the equilibrium

³i.e. the CG of payload itself, not of the loaded aircraft

Tank	Max. fuel capacity	
left wing	7375 L	(\approx 5900 kg of Jet A-1)
right wing	7375 L	(\approx 5900 kg of Jet A-1)
center	5250 L	(\approx 4200 kg of Jet A-1)

Table 2: Fuel tank capacity of VIRTAC-Castor

²in version 0.5-alpha and in version 0.52-beta as well

on the ground (with respect to the landing gear position, ensuring maneuverability on ground, not overloading the respective landing gears, etc.) will also be included. This aircraft loading envelope would complement the flight envelope limits defined in the following section.

4 FIRST DEFINITION OF THE FLIGHT ENVELOPE

The VIRTAC-Castor flight envelope definition is orientated on the aircraft's foreseen operations as short to medium range transport aircraft. Several limitations of the flight envelope have already been defined in [41] and given in Table 1 with a few additions. These initial limits already included the maximum values for speed, altitude and aircraft mass: they were verified and kept (as there was no need to modify them) but are complemented hereafter for version 0.52-beta.

In particular, maximum velocities for each configuration were defined and are given hereafter. In the clean configuration, the maximum speed is limited by either of two values (whichever is reached first for the current atmospheric conditions): the maximum operating speed VMO is 300 kt CAS (calibrated airspeed) and the maximum operating Mach number MMO is 0.76.

Table 3 provides the values for the maximum velocity with flaps extended (VFE) for each of the high lift configurations, from 1 to 5 (full flaps). The high lift system can only be used at FL200 (20,000 ft) or below. This is rather an arbitrary value, which was inspired by the Airbus A320. Note that a steady horizontal flight is not expected to be possible with each of these configurations across all altitudes (from ground to FL200) and for all weights between OEW (operational empty weight) and MTOW (maximum take-off weight).

Whilst this does not constitute a real limit of the flight envelope, setting initial conditions with a velocity lower than the ones given in Table 4 will generate an error message. These boundaries will be refined in the future: they correspond to a first attempt at making VIRTAC-Castor behave like the aircraft plus its flight test pilots/engineers. If an experimenter defines a test card with flight conditions which include a very low velocity for the desired altitude and the expected aircraft mass, the flight test engineers or the pilots would normally reject that test point (refuse to even try to perform that maneuver). In VIRTAC-Castor v0.52-beta, the minimal velocities (see Table 4) are applied regardless of the current aircraft mass. The values given in this table should correspond to velocities that are slightly above the stall speed in 1g flight at MTOW ($V_{s1g}(m = MTOW)$). For larger altitudes the limits on the engines' thrust will probably prevent a successful trim in steady flight.

New cross-checks of the aircraft fuel and payload configurations were added. All in all, the current definition of the flight envelope allows a flight with operational aircraft mass configuration within its limits.

high lift configuration	max. altitude (flight level)	VFE(conf) in kt (CAS)
1	FL200	220
2	FL200	205
3	FL200	175
4	FL200	175
5 (full)	FL200	160

Table 3: Boundaries of VIRTAC-Castor flight envelope; high lift configuration 1 to 5 (full)

high lift conf.	0	1	2	3	4	5
V_{min} in kt (CAS)	195	180	170	165	155	145

Table 4: Additional limitation imposed on the initial minimum speed for VIRTAC-Castor for configuration 0 (clean) to 5 (full)

Users should keep in mind that the lower limit of the aircraft mass configuration for reasonable operations is a minimum fuel of 2000 kg and payload of 1000 kg, even if the model allows lower weights. As already mentioned earlier, VIRTAC-Castor users should keep in mind that the aircraft's performance does not allow a steady flight with MTOW throughout the whole envelope. Especially in case of a fully deployed high lift system, the maximum altitude for steady flight conditions is lower than the maximum altitude for extending flaps defined in Table 3. Figure 3 summarizes all the limits given in this section in an altitude-speed diagram.

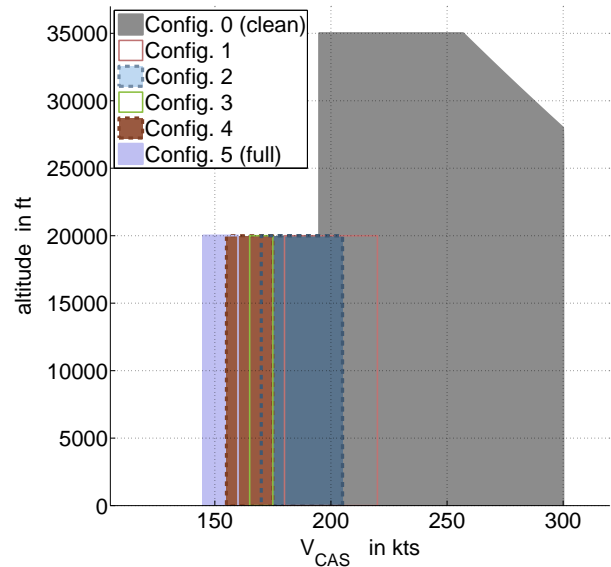


Figure 3: VIRTAC-Castor design flight envelope: altitude-speed diagram for different aircraft high lift system configurations.

5 NEW FAILURE CASES

For the first version of the benchmark model several test scenarios and failure cases are already available and will be extended in the future. The currently foreseen set of scenarios contains:

- wing icing
- horizontal tail damage and icing
- actuator faults
- engine bird strike

This section focuses on the failure cases that are added to VIRTAC-Castor in v0.52-beta: a wing icing case and an actuator jamming fault for elevators, ailerons and rudder.

5.1 WING ICE CASE

Ice can have hazardous effects on the aircraft's flight characteristics [45]. Large accumulations on the wing – usually mostly near the wing leading edge – increase the drag and reduce the maximum angle of attack (see Fig. 4) and consequently increase the stall speed. This has a direct influence on the safe flight envelope and poses a threat to crew and passengers. VIRTAC-Castor (and probably most future VIRTAC family models) will be capable of considering the effects of a generic wing ice accumulation in terms of the resulting aerodynamic degradation. The timely increase of degradation resp. accumulation as well as a de-icing can be triggered by the user whereas the details about the degradation itself are part of the closed model to allow a fair and realistic test of new developments like detection algorithms or robust flight controllers. The corresponding knowledge about the effects to be expected and a realistic amount of degradation is derived from previous icing research at DLR [46, 47] where high-quality simulation models were identified from flight data.

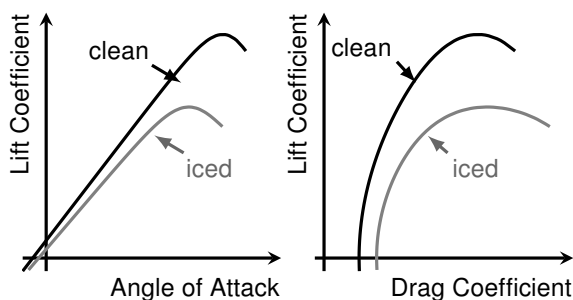


Figure 4: Change of aircraft lift curve and drag polar adapted from [45]

To reliably simulate the wing ice case several points must be considered. First, ice accumulation on the aircraft wings and other parts of the airframe occurs with specific atmospheric conditions which favor the existence of supercooled liquid water in the air. These conditions are normally found in clouds and therefore are

accompanied by a significant level of turbulence. In the VIRTAC model this is considered by enforcing a minimum level of turbulence when the wing ice case is active (activation and deactivation occur with some random time delay between a few seconds and one minute).

Second, the existence of certain icing conditions in the atmosphere is still hard to predict due to the complex stochastic effects. Nevertheless, areas with a high probability of icing conditions can be predicted nowadays. The fact that we are dealing with probabilities of encountering icing conditions also means that icing in VIRTAC should not start instantaneously after triggering the wing ice case flag. As this new failure case might be of interest for scientists/engineers who are working on ice detection or on flight control adaption/reconfiguration, the implementation includes some randomness. For instance, the actual simulated ice accretion and as a consequence the change of aerodynamics characteristics of VIRTAC-Castor start with a random time delay.

Third, ice accretion is in general a relatively slow process (compared to the typical airplane dynamics), except for a flight in special rare atmospheric conditions. For VIRTAC-Castor, a model covering the major effects of icing in the most general case is implemented which considers a moderate ice accretion rate. On the other hand, when resetting the wing ice case (e.g. to simulate the activation of an ice protection system), a near to nominal behavior is obtained fairly quickly.

Figure 5 shows the results of an example simulation with temporary wing ice. In this specific example, in order to allow a stable flight during this relatively long simulation of the aircraft motion with increasing aerodynamic degradation a very simple controller is used to maintain the altitude. Nevertheless, it was decided to not use an additional speed control loop which allows to see the icing-induced flight performance change in a reduction of the airspeed. After 50 s of steady state horizontal flight, the wing ice flag is triggered to initiate the failure case. Several seconds later the measured pitch rate shows the aircraft's response to the medium turbulence which accompanies the icing in the VIRTAC-Castor model by definition⁴. After some additional (random) time delay, the aircraft's aerodynamic characteristics start to change, which typically consists in a deterioration of the flight performance as well as further changes affecting the dynamic behavior and the handling of the aircraft. The simple controller in this example compensates the loss of altitude, which would otherwise occur, with a counteracting elevator command. Consequently, the loss of total energy due to the performance deterioration can be seen through the loss of kinetic energy. The reset of the original aircraft aerodynamics is triggered by removing the failure case flag at 430 s of simulation time. The aircraft "leaves" the icing

⁴Note that the turbulence is barely visible in the measured angle of attack and airspeed resulting from the implemented sensor characteristics and amplitude of measurement noise.

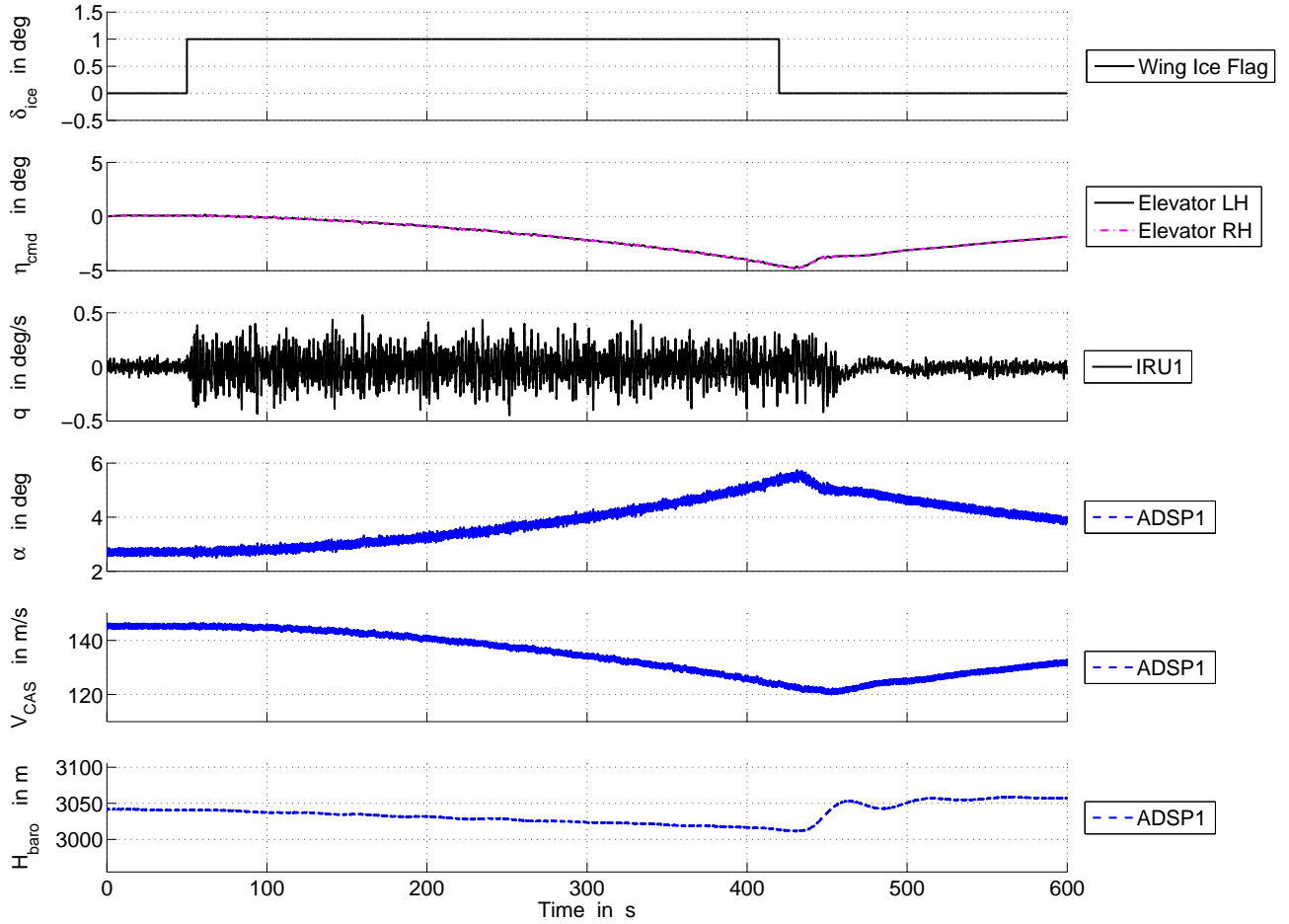


Figure 5: Example of wing ice case with VIRTAC-Castor: time histories of wing ice case flag, commanded elevator deflection (LH/RH) aircraft pitch response, measured angle of attack, measured calibrated airspeed and measured barometric altitude.

conditions, the deterioration of the aircraft aerodynamics characteristics is removed within a random time frame and additional turbulence is stopped after the wing ice failure case is completely reset inside the model.

The herein presented wing icing scenario already includes very interesting effects and is a capability that is otherwise not available in other freely distributed flight dynamics models. The authors intend to further improve the modeling of wing icing, for instance by including asymmetric ice shapes as well as by improving the aerodynamic model for symmetric ice shapes during asymmetric flight (e.g. asymmetric stall during lateral maneuvers). Such capabilities were already developed by the authors for other models, but need to be ported to VIRTAC-Castor.

5.2 ACTUATOR JAMMING

In the long term the authors intend to develop and integrate very realistic actuator models, which include many real-world effects related to the variations in terms of dynamic behavior for the nominal (i.e. fully functioning) actuators but also in faulty conditions. In version 0.52-beta

the implementation of the actuators has been modified to prepare for the future inclusion of these real-world effects and an actuator jamming, i.e. “freezing” of one or more actuators, is made available as a first (simple) fault case. Note that the actuator position measurement remains affected by noise and is therefore not constant. The primary control surface actuators of both elevators, ailerons and the rudder can be set in failure mode, which will trigger the jamming fault at the current position within a certain time delay (less than 30 seconds) after receiving the fault flag in the model. As VIRTAC is meant to be a very realistic virtual flight test platform the actuator fault is initialized randomly after triggering the failure case because such failure would occur unforeseeable in a real aircraft. Resetting the actuator and restoring the normal behavior is also done randomly within a certain time frame after removing the failure case flag.

Figure 6 gives an example of separate actuator faults of left and right elevator. For this example an elevator sweep input command of small amplitude is used to visualize the failure case characteristics. The jamming of the two actuators (of the left and of the right elevators)

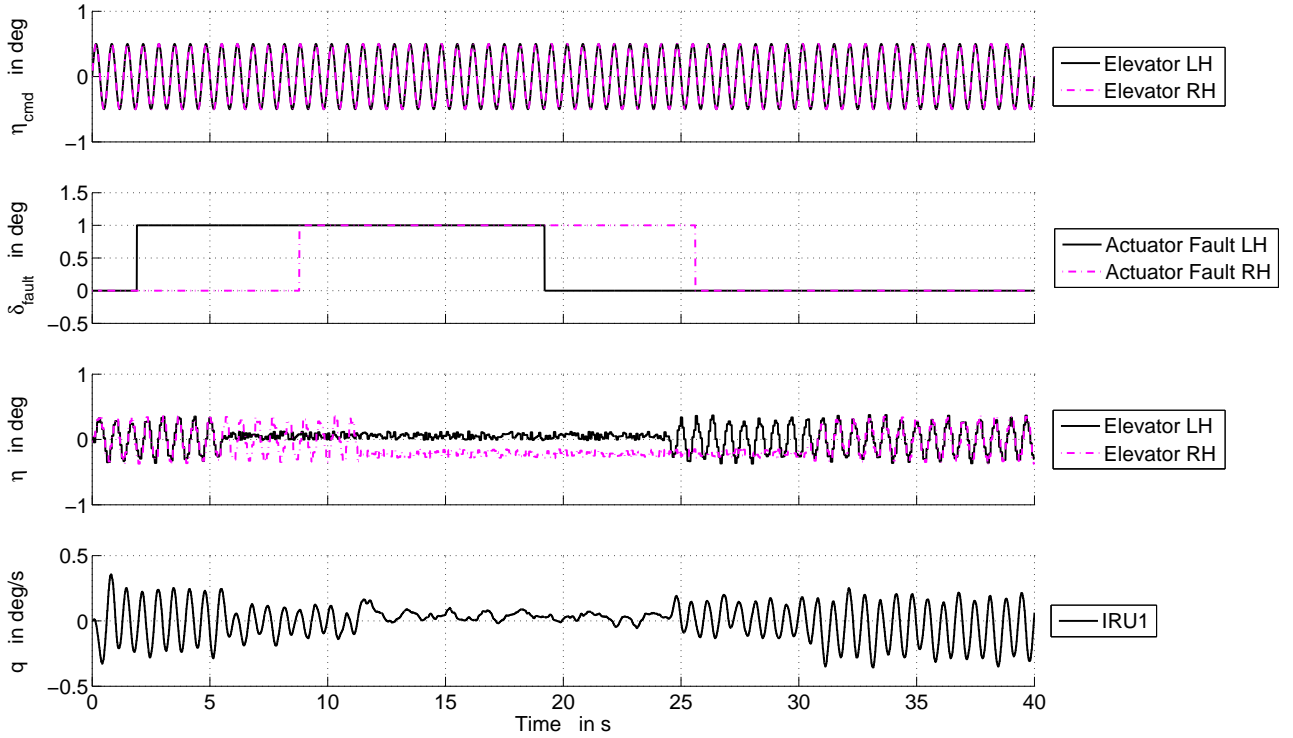


Figure 6: Example of elevator actuator jamming with VIRTAC-Castor: time histories of commanded elevator deflection (LH/RH), measured elevator deflection (LH/RH), aircraft pitch response and actuator fault flags for both elevator actuators.

is triggered and reset at different – arbitrarily chosen – simulation times:

- left hand elevator actuator jamming:
provoked at 1.9 s and reset at 19.2 s,
- right hand elevator actuator jamming:
provoked at 8.8 s and reset at 25.6 s.

As for the wing icing case, the flag does not trigger the fault directly but rather configures the simulation in such a way that the fault will occur in the near future. The change in behavior of the actuator will occur several seconds after the flag was set: the delay is here also random. When this happens the control surface stops at the current position. With the frozen left hand elevator, the output of the VIRTAC-Castor model changes accordingly in terms of reducing the dynamic pitch rate response amplitude by 50 % (measured signal from IRU1). During the phase of both actuators frozen, the commanded sweep input is not fed to the control surface. After resetting the actuator faults, the actuators work properly again and the aircraft reacts perfectly to the elevator input sweep.

This very simple fault presented here is just a prelude to the introduction of many more real-world effects into the VIRTAC actuator models. It also illustrates the kind of triggering mechanisms that the authors are currently considering for implementing benchmarks based on VIRTAC and involving complex combination of faults. This reduced capability can already be used

to demonstrate controllers with automatic reallocation of the control commands.

6 SUMMARY

This paper presents the ongoing developments of the VIRTAC-Castor model that the authors created and made available to the entire community this year via GitHub. At this stage, this activity is a side project for the authors with very limited resources, but the authors are convinced that sharing these models and developing good benchmarks around them can be very valuable for the aircraft flight dynamics and control community. The current developments focus on three areas: 1) further validation and refinement of the models provided, 2) development of concrete scenarios for benchmarks, and 3) continuous improvement of the underlying code base in order to permit quick update cycles and prepare for more complex models. This third aspect is hardly observable from the users' point of view but is presently where most of the work is being done. Indeed, the requirements that are specific to VIRTAC and linked to ensuring that the model can only be used as a test aircraft could require the implementation of mechanisms that are otherwise not needed in typical models / simulation programs.

References

- [1] T. Lombaerts, G. Looye, J. Ellerbroek, and M. Rodriguez y Martin, "Design and piloted simulator evaluation of adaptive safe flight envelope protection algorithm," *Journal of Guidance, Control, and Dynamics*, vol. 40, no. 8, pp. 1902–1924, August 2017. DOI: [10.2514/1.G002525](https://doi.org/10.2514/1.G002525).
- [2] T. Lombaerts, G. Looye, P. Chu, and J. A. Mulder, "Pseudo control hedging and its application for safe flight envelope protection," in *Proceedings of the 2010 AIAA Guidance, Navigation, and Control Conference*, (Toronto, ON, Canada), August 2nd–5th 2010. AIAA 2010-8280.
- [3] C. Tomlin, J. Lygeros, and S. Sastry, "Aerodynamic envelope protection using hybrid control," in *Proceedings of the 1998 American Control Conference*, (Philadelphia, PA, USA), IEEE, June 1998. DOI: [10.1109/ACC.1998.707322](https://doi.org/10.1109/ACC.1998.707322).
- [4] H.-H. Shin, S.-H. Lee, Y. Kim, E.-T. Kim, and K.-J. Sung, "Design of a flight envelope protection system using a dynamic trim algorithm," *International Journal of Aeronautical and Space Sciences*, vol. 12, no. 3, pp. 241–251, September 2011. DOI: [10.5139/IJASS.2011.12.3.241](https://doi.org/10.5139/IJASS.2011.12.3.241).
- [5] K. H. Well, "Aircraft control laws for envelope protection," in *Proceedings of the AIAA Guidance, Navigation, and Control Conference and Exhibit*, (Keystone, CO, USA), August 21st–24th 2006. AIAA 2006-6055.
- [6] M. Rafi, J. E. Steck, and K. Rokhsaz, "A microburst response and recovery scheme using advanced flight envelope protection," in *Proceedings of the AIAA Guidance, Navigation, and Control and Co-located Conferences*, (Minneapolis, MN, USA), August 13th–16th 2012. AIAA 2012-4444.
- [7] J. M. Wilson and M. E. Peters, "Automatic flight envelope protection for light general aviation aircraft," in *Proceedings of the 28th Digital Avionics Systems Conference*, (Orlando, FL, USA), October 23rd–29th 2009. DOI: [10.1109/DASC.2009.5347458](https://doi.org/10.1109/DASC.2009.5347458).
- [8] K. N. Hossain, V. Sharma, M. B. Bragg, and P. G. Voulgaris, "Envelope protection and control adaptation in icing encounters," in *Proceedings of the 41st Aerospace Sciences Meeting and Exhibit*, (Reno, NV, USA), January 6th–9th 2003. AIAA 2003-25.
- [9] D. R. Gingras, B. P. Barnhart, R. J. Ranuado, T. P. Ratvasky, and E. A. Morelli, "Envelope protection for in-flight ice contamination," in *Proceedings of the 47th AIAA Aerospace Sciences Meeting*, (Orlando, FL, USA), January 5th–8th 2009. AIAA 2009-1458.
- [10] N. Tekles, F. Holzapfel, E. Xargay, R. Choe, N. Hovakimyan, and I. M. Gregory, "Flight envelope protection for NASA's transport class model," in *Proceedings of the AIAA 2014 SciTech - Guidance, Navigation, and Control Conference*, (National Harbor, MD, USA), January 13th–17th 2014. AIAA 2014-0269.
- [11] K. A. Ackerman, D. A. Talleur, R. S. Carbonari, E. Xargay, B. D. Seefeldt, A. Kirlik, N. Hovakimyan, and A. C. Trujillo, "Automation situation awareness display for a flight envelope protection system," *Journal of Guidance, Control, and Dynamics*, vol. 40, no. 4, pp. 964–980, 2017. DOI: [10.2514/1.G000338](https://doi.org/10.2514/1.G000338).
- [12] N. Tekles, J. Chongvisal, E. Xargay, R. Choe, D. A. Talleur, N. Hovakimyan, and C. M. Belcastro, "Design of a flight envelope protection system for NASA's transport class model," *Journal of Guidance, Control, and Dynamics*, vol. 40, no. 4, pp. 863–877, 2017. DOI: [10.2514/1.G001728](https://doi.org/10.2514/1.G001728).
- [13] L. Tang, M. Roemer, J. Ge, A. Crassidis, J. V. R. Prasad, and C. Belcastro, "Methodologies for adaptive flight envelope estimation and protection," in *Proceedings of the AIAA Guidance, Navigation, and Control Conference*, (Chicago, IL, USA), August 10th–13th 2009. AIAA 2009-6260.
- [14] D. R. Gingras, B. Barnhart, R. Ranaudo, B. Martos, T. P. Ratvasky, and E. Morelli, "Development and implementation of a model-driven envelope protection system for in-flight ice contamination," in *Proceedings of the 2010 AIAA Guidance, Navigation, and Control Conference*, (Toronto, ON, Canada), August 2nd–5th 2010. AIAA 2010-8141.
- [15] W. Falkena, C. Borst, Q. P. Chu, and J. A. Mulder, "Investigation of practical flight envelope protection systems for small aircraft," *Journal of Guidance, Control, and Dynamics*, vol. 34, no. 2, pp. 976–988, July 2011. DOI: [10.2514/1.53000](https://doi.org/10.2514/1.53000).
- [16] H. Ye, M. Chen, and Q. Wu, "Flight envelope protection control based on reference governor method in high angle of attack maneuver," *Mathematical Problems in Engineering*, vol. 2015, Article ID 254975, p. 15, 2015. DOI: [10.1155/2015/254975](https://doi.org/10.1155/2015/254975).
- [17] A. A. Lambregts, "Flight envelope protection for automatic and augmented manual control," in *Proceedings of the EuroGNC 2013, 2nd CEAS Specialist Conference on Guidance, Navigation & Control*, (Delft, The Netherlands), pp. 1364–1383, April 10th–12th 2013.
- [18] V. Klein, "Aircraft parameter estimation in frequency domain," in *Proceeding of the 4th Atmospheric Flight Mechanics Conference*, (Palo Alto, CA, USA), August 7th–9th 1978. AIAA 1978-1344.

- [19] E. A. Morelli and V. Klein, "Optimal input design for aircraft parameter estimation using dynamic programming principles," in *Proceedings of the 17th Atmospheric Flight Mechanics Conference*, (Portland, OR, USA), August 20th-22th 1990. [AIAA-90-2801](#).
- [20] P. Lichota, K. Sibilski, and P. Ohme, "D-optimal simultaneous multistep excitations for aircraft parameter estimation," *Journal of Aircraft*, vol. 54, no. 2, pp. 747–758, March 2017. [DOI: 10.2514/1.C033794](#).
- [21] J. R. Raol and R. V. Jategaonkar, "Aircraft parameter estimation using recurrent neural networks - A critical appraisal," in *20th Atmospheric Flight Mechanics Conference, Guidance, Navigation, and Control and Co-located Conferences*, (Baltimore, MD, USA), August 7th-10th 1995. [AIAA-95-3504](#).
- [22] R. V. Jategaonkar and F. Thielecke, "Aircraft parameter estimation – a tool for development of aerodynamic databases," *Sadhana*, vol. 25, pp. 119–135, April 2000. [DOI: 10.1007/BF02703754](#).
- [23] R. V. Jategaonkar and E. Plaetschke, "Algorithms for aircraft parameter estimation accounting for process and measurement noise," *Journal of Aircraft*, vol. 26, no. 4, pp. 360–372, April 1989. [DOI: 10.2514/3.45769](#).
- [24] R. Jategaonkar, D. Fischenberg, and W. von Gruenhagen, "Aerodynamic modeling and system identification from flight data-recent applications at DLR," *Journal of Aircraft*, vol. 41, no. 4, pp. 681–691, July-August 2004. [DOI: 10.2514/1.3165](#).
- [25] K. W. Iliff, "Aircraft parameter estimation," in *Proceedings of the 25th AIAA Aerospace Sciences Meeting*, (Reno, NV, USA), January 12th-15th 1987. [AIAA 1987-0623](#).
- [26] P. R. Chandler, M. Pachter, and M. Mears, "System identification for adaptive and reconfigurable control," *Journal of Guidance, Control, and Dynamics*, vol. 18, no. 3, pp. 516–524, May 1995. [DOI: 10.2514/3.21417](#).
- [27] E. A. Morelli, "In-flight system identification," in *Proceedings of the 23rd Atmospheric Flight Mechanics Conference*, (Boston, MA, USA), August 10th-12th 1998. [AIAA-98-4261](#).
- [28] E. A. Morelli, "Practical aspects of the equation-error method for aircraft parameter estimation," in *AIAA Atmospheric Flight Mechanics Conference*, (Keystone, CO, USA), August 21st-24th 2006. [AIAA 2006-6144](#).
- [29] N. K. Peyada and A. K. Ghosh, "Aircraft parameter estimation using a new filtering technique based upon a neural network and Gauss-Newton method," *The Aeronautical Journal*, vol. 113, no. 1142, pp. 243–252, April 2009. [DOI: 10.1017/S0001924000002918](#).
- [30] N. K. Peyada and A. K. Ghosh, "Aircraft parameter estimation using neural network based algorithm," in *Proceedings of the 2009 AIAA Atmospheric Flight Mechanics Conference*, (Chicago, IL, USA), August 10th-13th 2009. [AIAA 2009-5941](#).
- [31] G. Chowdhary and R. Jategaonkar, "Aerodynamic parameter estimation from flight data applying extended and unscented Kalman filter," *Aerospace Science and Technology*, vol. 14, no. 2, pp. 106–117, March 2010. [DOI: 10.1016/j.ast.2009.10.003](#).
- [32] E. A. Morelli, "Flight test maneuvers for efficient aerodynamic modeling," *Journal of Aircraft*, vol. 49, no. 6, pp. 1857–1867, Nov. 2012. [DOI: 10.2514/1.C031699](#).
- [33] E. A. Morelli and V. Klein, "Application of system identification to aircraft at nasa langley research center," *Journal of Aircraft*, vol. 42, no. 1, pp. 12–25, January 2005. [DOI: 10.2514/1.3648](#).
- [34] A. Dorobantu, A. Murch, B. Mettler, and G. Balas, "System identification for small, low-cost, fixed-wing unmanned aircraft," *Journal of Aircraft*, vol. 50, no. 4, pp. 1117–1130, July 2013. [DOI: 10.2514/1.C032065](#).
- [35] A. Fujimori and L. Ljung, "A polytopic modeling of aircraft by using system identification," in *Proceeding of the 2005 International Conference on Control and Automation*, (Budapest, Hungary), IEEE, June 27th-29th 2005. [DOI: 10.1109/ICCA.2005.1528100](#).
- [36] A. Fujimori and L. Ljung, "Model identification of linear parameter varying aircraft systems," *Journal of Aerospace Engineering*, vol. 220, no. 4, pp. 337–346, 2006. [DOI: 10.1243/09544100JAERO28](#).
- [37] M. Jamil and X.-S. Yang, "A literature survey of benchmark functions for global optimization problems," *Int. Journal of Mathematical Modelling and Numerical Optimisation*, vol. 4, no. 2, pp. 150–194, May 2013. [DOI: 10.1504/IJMMNO.2013.055204](#).
- [38] R. M. Hueschen, *Development of the Transport Class Model (TCM) Aircraft Simulation From a Sub-Scale Generic Transport Model (GTM) Simulation*. Technical Memorandum, National Aeronautics and Space Administration, Hampton, VA, USA, August 2011.
- [39] N. T. Frink, S. Z. Pirzadeh, H. L. Atkins, S. A. Viken, and J. H. Morrison, "CFD assessment of aerodynamic degradation of a subsonic transport due to

airframe damage,” in *Proceedings of the 2010 AIAA Aerospace Science Meeting*, (Orlando, FL, USA), January 2010. [AIAA 2010-500](#).

- [40] N. Fezans and C. Deiler, “Generation of a dataset for system identification with VIRTAC-Castor,” in *Proceedings of the 2019 German Aerospace Congress (DLRK)*, (Darmstadt, Germany), Sept.-Oct. 2019.
- [41] C. Deiler and N. Fezans, “VIRTAC - a family of virtual test aircraft for use in flight mechanics and GNC benchmarks,” *Proceedings of the 2019 AIAA Scitech - Intelligent Systems Conference*, (San Diego, CA, USA), Jan. 2019. [AIAA 2019-0950](#).
- [42] D. Fischenberg, “Identification of an unsteady aerodynamic stall model from flight test data,” in *Proceedings of the 1995 AIAA Atmospheric Flight Mechanics Conference*, (Baltimore, MD, USA), pp. 138–146, Aug. 7-10 1995. [AIAA 95-3438-CP](#).
- [43] D. Fischenberg and R. V. Jategaonkar, “Identification of aircraft stall behavior from flight test data,” in *RTO Systems Concepts and Integration Panel (SCI) Symposium: System Identification for Integrated Aircraft Development and Flight Testing*, no. 17, (Madrid, Spain), NATO Research and Technology Organisation, May 5th - 7th 1998.
- [44] N. Fezans and C. Deiler, “Inside the virtual test aircraft (VIRTAC) benchmark model: Simulation architecture,” *Simulation Notes Europe (SNE)*, vol. 29, no. 1, pp. 1–12, 2019. [DOI: 10.11128/sne.29.on.10461](#).
- [45] N. N., “Ice accretion simulation,” AGARD Advisory Report 344, Advisory Group for Aerospace Research & Development (AGARD) - Fluid Dynamics Panel Working Group 20, North Atlantic Treaty Organization (NATO), Neuilly-Sur-Seine, France, December 1997.
- [46] C. Deiler, “Time domain output error system identification of iced aircraft aerodynamics,” *CEAS Aeronautical Journal*, vol. 8, no. 2, pp. 231–244, June 2017. [DOI: 10.1007/s13272-016-0231-2](#).
- [47] C. Deiler, “Aerodynamic modeling, system identification, and analysis of iced aircraft configurations,” *Journal of Aircraft*, vol. 55, no. 1, pp. 145–161, January-February 2018. [DOI: 10.2514/1.C034390](#).

A CONDITIONS OF USE

The following information is provided with the aim of allowing the readers of the paper to know the terms of the used licenses without having to download VIRTAC first. Since these licenses might evolve over time and differ from file to file, the license information provided with each VIRTAC model applies: the following information is of indicative nature only.

Source files

As of now, anyone can download and use the VIRTAC models. Any part of VIRTAC provided in source form (e.g. MATLAB .m files or Simulink models) is subject to the very permissive MIT license:

MIT License

Copyright (c) 2018 Deutsches Zentrum für Luft- und Raumfahrt e.V., Christoph Deiler, Nicolas Fezans

Permission is hereby granted, free of charge, to any person obtaining a copy of this software and associated documentation files (the "Software"), to deal in the Software without restriction, including without limitation the rights to use, copy, modify, merge, publish, distribute, sublicense, and/or sell copies of the Software, and to permit persons to whom the Software is furnished to do so, subject to the following conditions:

The above copyright notice and this permission notice shall be included in all copies or substantial portions of the Software.

THE SOFTWARE IS PROVIDED "AS IS", WITHOUT WARRANTY OF ANY KIND, EXPRESS OR IMPLIED, INCLUDING BUT NOT LIMITED TO THE WARRANTIES OF MERCHANTABILITY, FITNESS FOR A PARTICULAR PURPOSE AND NONINFRINGEMENT. IN NO EVENT SHALL THE AUTHORS OR COPYRIGHT HOLDERS BE LIABLE FOR ANY CLAIM, DAMAGES OR OTHER LIABILITY, WHETHER IN AN ACTION OF CONTRACT, TORT OR OTHERWISE, ARISING FROM, OUT OF OR IN CONNECTION WITH THE SOFTWARE OR THE USE OR OTHER DEALINGS IN THE SOFTWARE.

Other files: executable, binaries, binary data

All non-disclosed code and data files (e.g. executable, dynamic/static libraries, binary files, etc.) are licensed under the Creative Commons Attribution-NoDerivs 4.0 Generic license (CC-BY-ND 4.0). A human-readable summary is provided hereafter: please refer to the official license text for the legally binding text. Note that any

attempt to disassemble the binary code, binary data, executable, or dynamic/static libraries provided is hereby considered as a derivative and is consequently hereby prohibited, even if not shared. A normal use of VIRTAC for its intended purpose does not require such operations and therefore users will normally not be affected by this restriction.

CC-BY-ND 4.0 *(human-readable summary)*

• You are free to:

- Share – copy and redistribute the material in any medium or format for any purpose, even commercially.
- The licensor cannot revoke these freedoms as long as you follow the license terms.

• Under the following terms:

- Attribution – You must give appropriate credit, provide a link to the license, and indicate if changes were made. You may do so in any reasonable manner, but not in any way that suggests the licensor endorses you or your use.
- NoDerivatives – If you remix, transform, or build upon the material, you may not distribute the modified material.
- No additional restrictions – You may not apply legal terms or technological measures that legally restrict others from doing anything the license permits.

B VIRTAC DOWNLOAD AND CONTACT INFORMATION

To provide the models of the VIRTAC family to the community, a GitHub repository was created. This repository is located at <https://github.com/VIRTAC/VIRTAC> and will be updated if necessary due to new model developments of aircraft within the VIRTAC family.

For any questions on VIRTAC-Castor, the VIRTAC family or for general support concerning the VIRTAC simulation, please use the following VIRTAC email address:

VIRTAC@dlr.de.